Wildtype allele

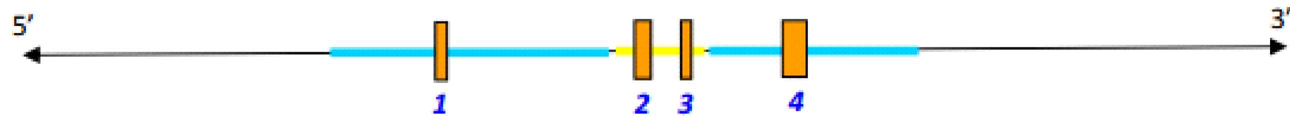

Targeting Vector

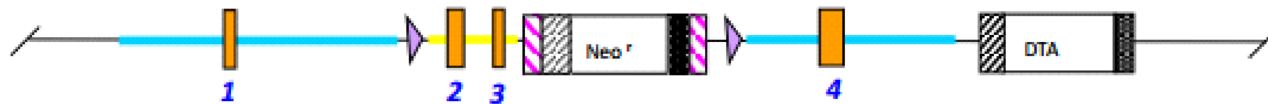

Targeted allele

Conditional KO allele
(after Flp recombination)

Constitutive KO allele
(after Cre recombination)

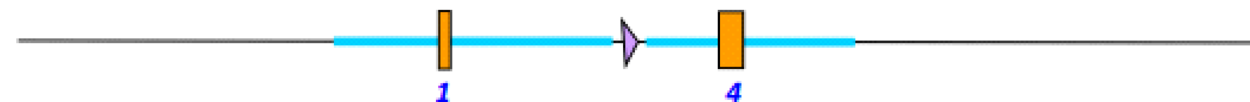

S1. Targeting strategy for generation of β2M$^{flox/flox}$ mice.

A.

Cell Type	WT (n=5)	Plt-β2M$^{-/-}$ (n=7)
WBC	12.6 ± 3	12.4 ± 2.5
Lymphocytes	9.8 ± 3.5	10.3 ± 1.7
Monocytes	0.46 ± 0.2	0.31 ± 0.14
Neutrophils	2.4 ± 0.6	2.0 ± 0.7
RBC	10.6 ± 0.5	10.6 ± 0.3
Platelets	524 ± 98	592 ± 98

B.

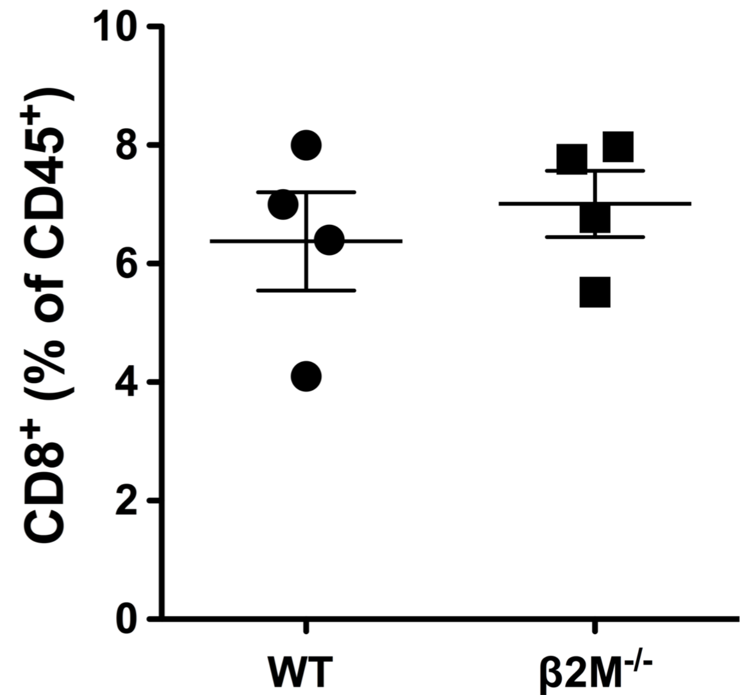

S2. WT and Plt-β2M$^{-/-}$ mice have similar A) leukocyte (N=5 WT, N=7 Plt-β2M$^{-/-}$, ± SEM, unpaired two-tailed t-test with Welch's correction) and B) circulating CD8^{+} T cell numbers (± SEM, unpaired two-tailed t-test with Welch's correction).

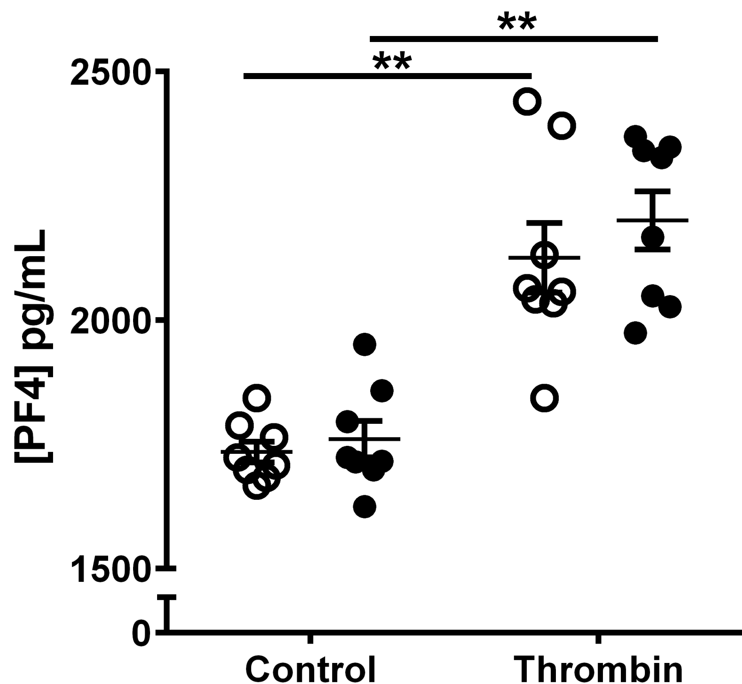

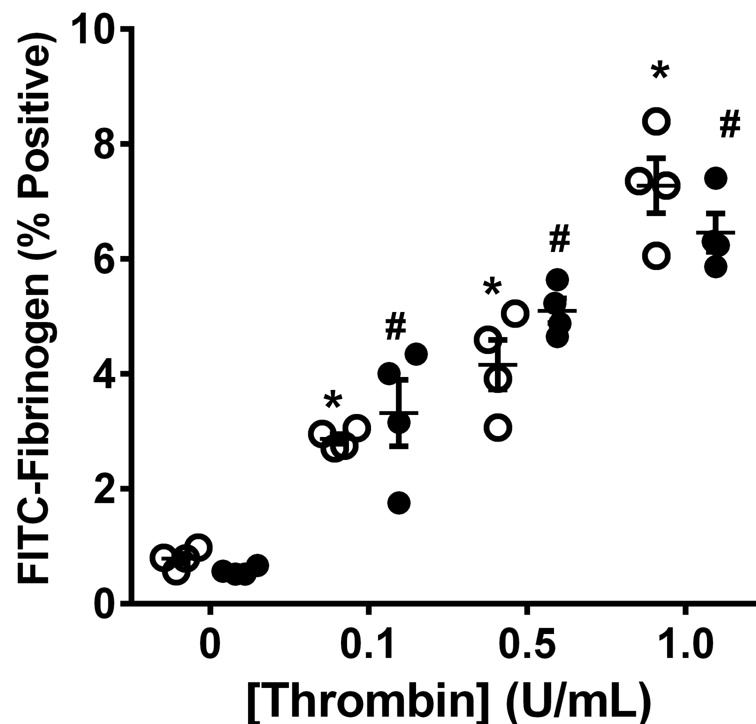

S3. Platelets from WT and Plt-β2M$^{-/-}$ mice had similar A) PF4 release (± SEM, *P<0.05, one-way ANOVA with Bonferroni correction) and B) fibrinogen binding (± SEM, *P<0.05 vs WT 0, #P<0.05 vs Plt-β2M$^{-/-}$ 0, one-way ANOVA with Bonferroni correction).

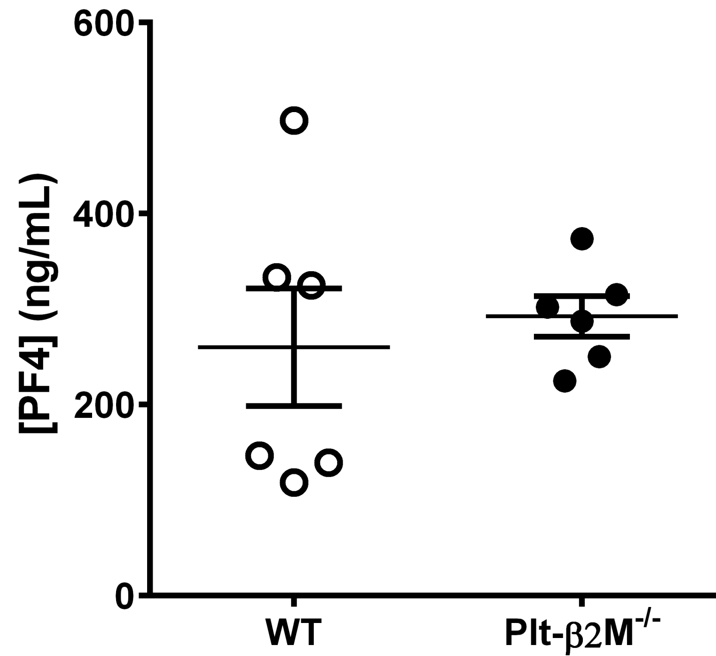

S4. WT and Plt-β2M$^{-/-}$ mice had similar plasma PF4 (± SEM, unpaired two-tailed t-test with Welch's correction).

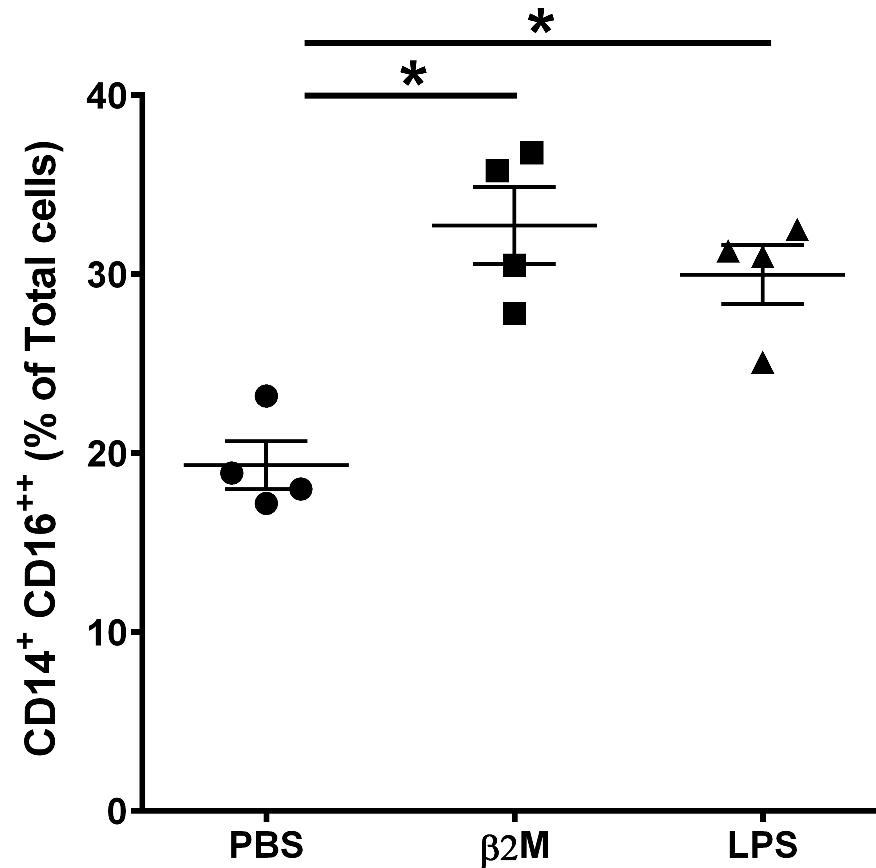

S5. β2M increased THP-1 CD16 expression. THP-1 cells were treated with control PBS, β2M (5 μg/mL), or LPS (10 ng/mL; ± SEM, *$P<0.05$, one-way ANOVA with Bonferroni correction).

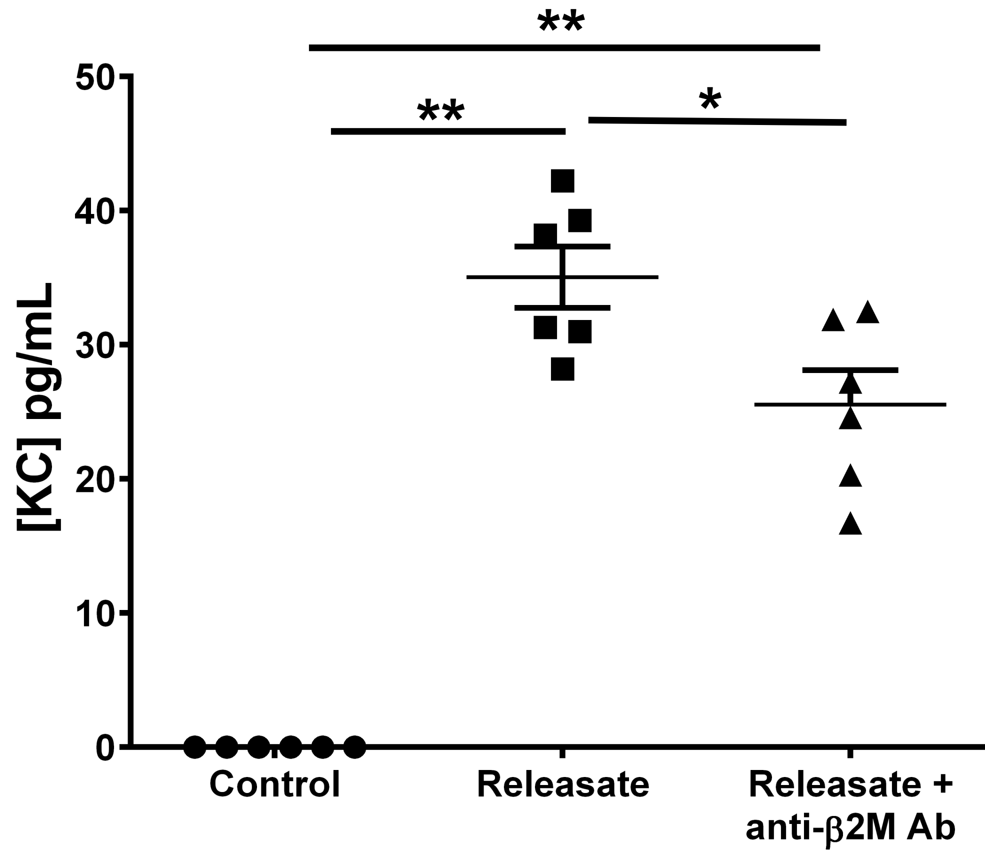

Fig S6. Anti-β2M antibody reduced platelet releasate induced monocyte KC production (± SEM, *P<0.05, *P<0.01, one-way ANOVA with Bonferroni correction).

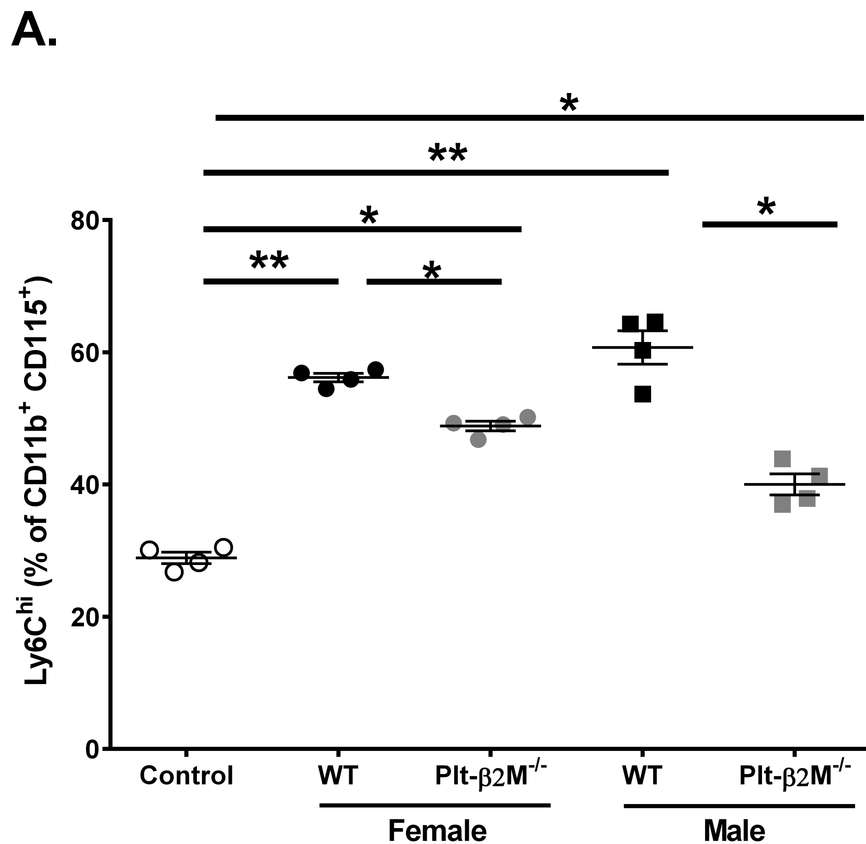

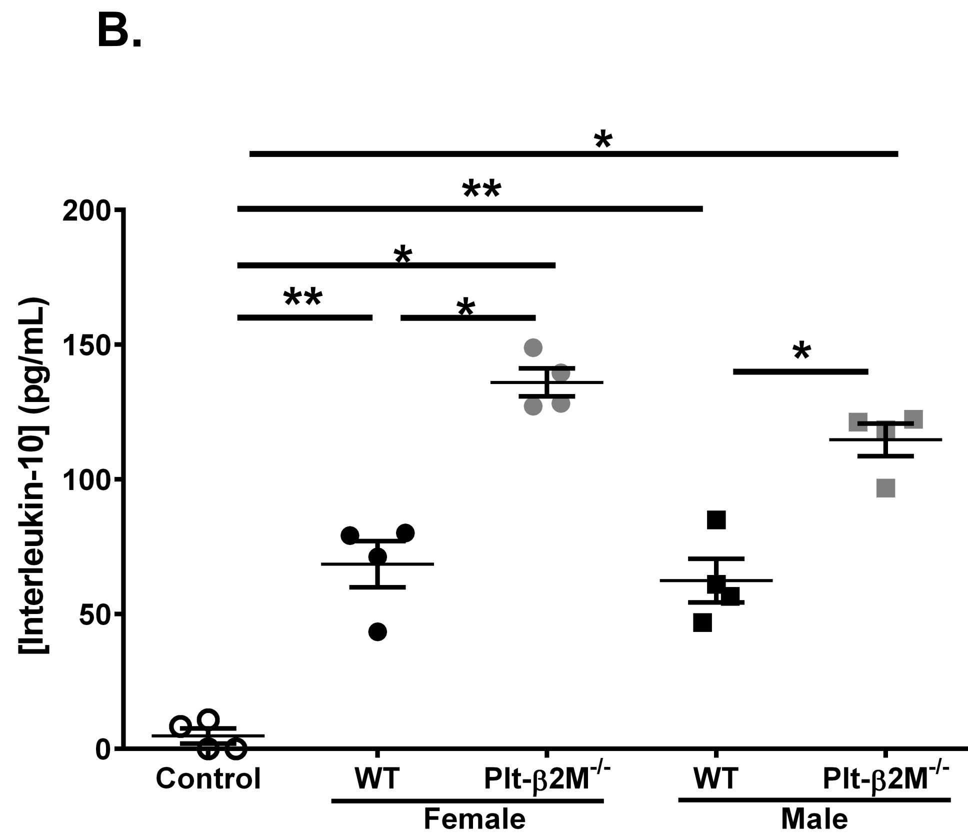

Fig S7. Platelets from male and female WT and Plt-β2M$^{-/-}$ mice induce similar monocyte responses as measured by A) surface Ly6C expression (± SEM, *P<0.05, **P<0.01, one-way ANOVA with Bonferroni correction) and B) IL-10 release (± SEM, *P<0.05, **P<0.01, one-way ANOVA with Bonferroni correction).

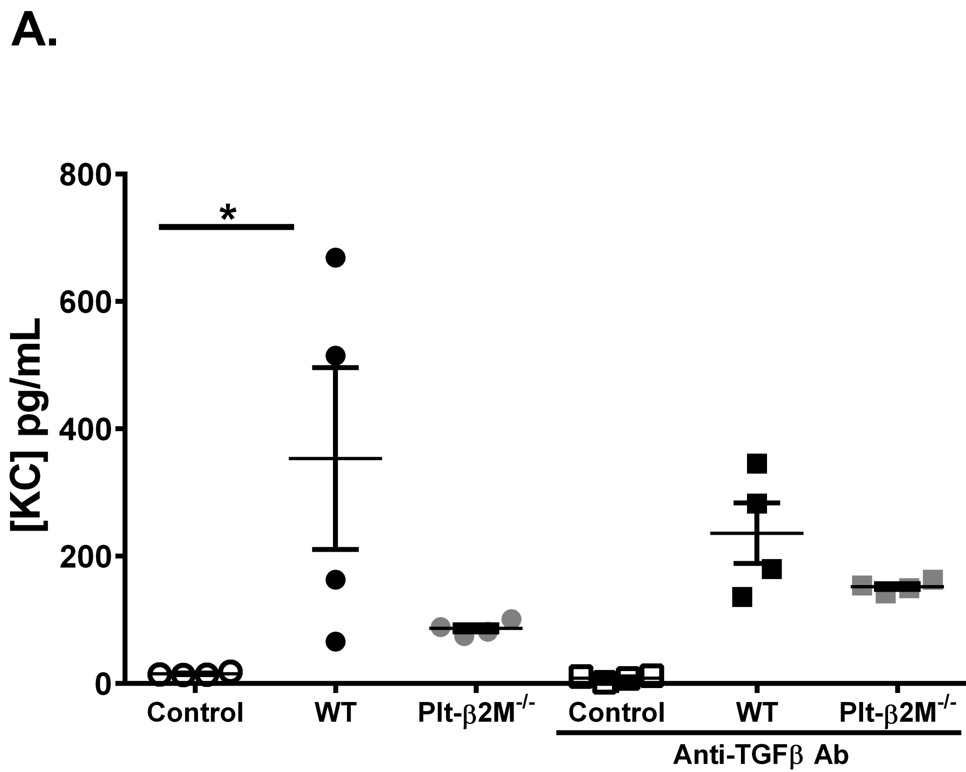

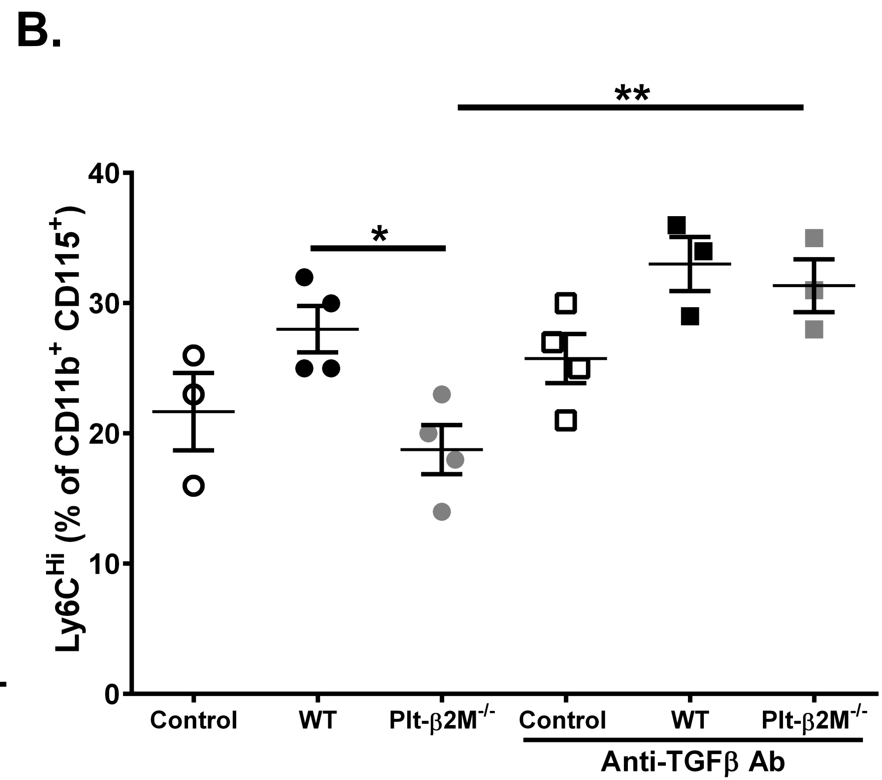

Fig S8. WT and Plt-β2M$^{-/-}$ releasate treated with anti-TGFβ antibody had similar A) KC release (± SEM, *$P<0.05$, one-way ANOVA with Bonferroni correction) and B) Ly6C^{hi} monocyte polarization (± SEM, *$P<0.05$, **$P<0.01$, one-way ANOVA with Bonferroni correction). Mouse monocytes (50,000/well) were incubated with the releasate from WT or plt-β2M$^{-/-}$ mouse platelets (10:1 ratio platelet:monocyte) for 48 hr.

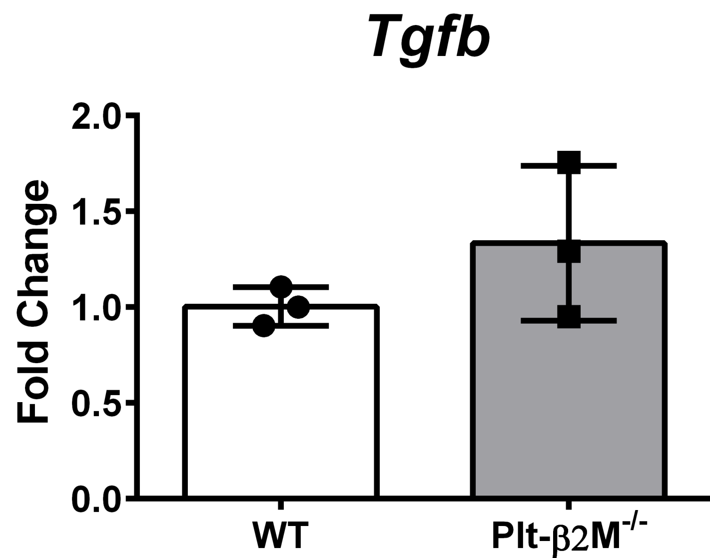

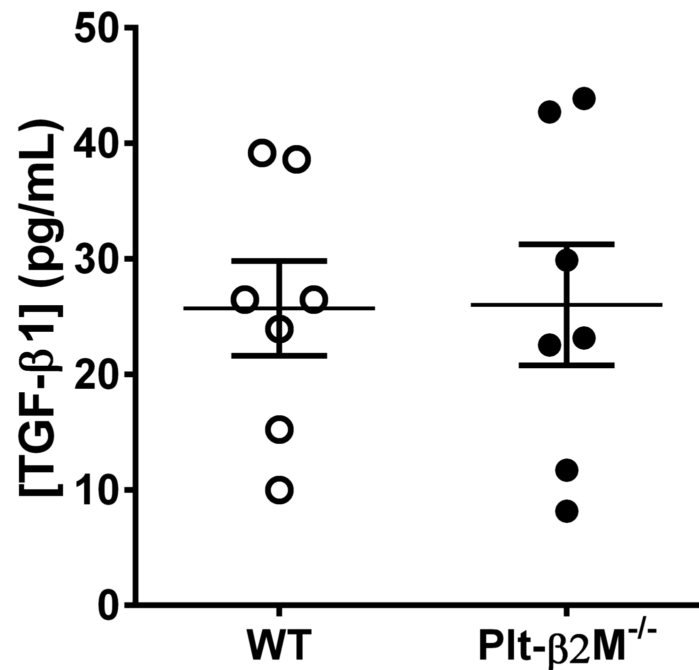

Fig S9. WT and Plt-β2M$^{-/-}$ platelets had similar TGFβ content. A) Platelet *Tgfb* mRNA quantified by qRT-PCR (± SEM, unpaired two-tailed t-test with Welch's correction) and B) TGFβ release from thrombin (1 U/mL) stimulated platelets quantified by ELISA (± SEM, unpaired two-tailed t-test with Welch's correction) .

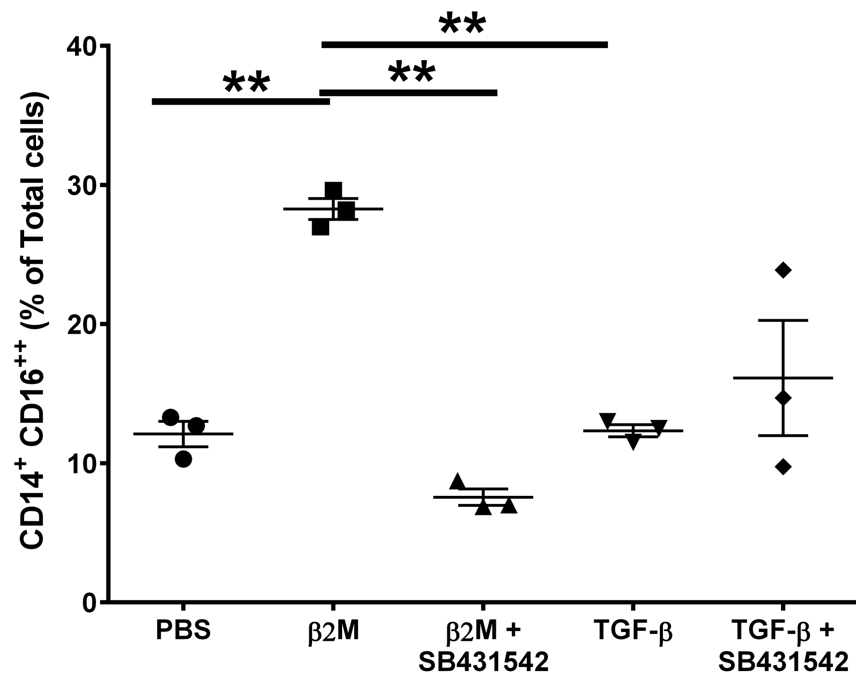

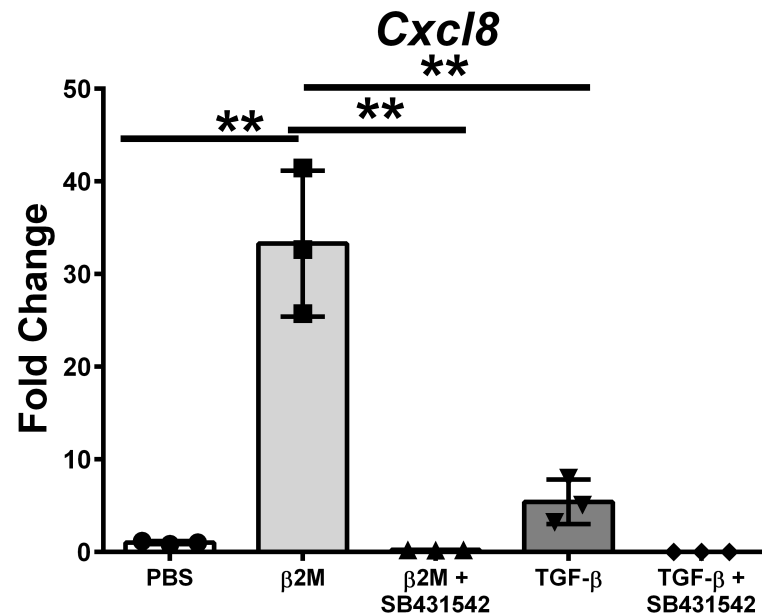

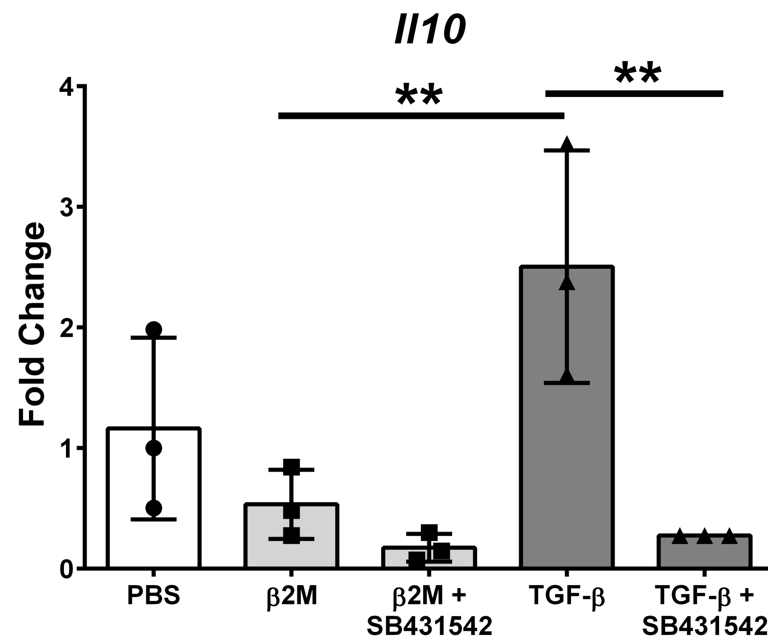

S10. TGFβR inhibitor prevents β2M and TGFβ induced THP-1 polarization. A) CD16 expression was measured by flow cytometry (± SEM, $^{**}P<0.01$ one-way ANOVA with Bonferroni correction). B) *IL8* and *IL10* RNA expression was determined by qRT-PCR (± SD, $^{**}P<0.01$, one-way ANOVA with Bonferroni correction).

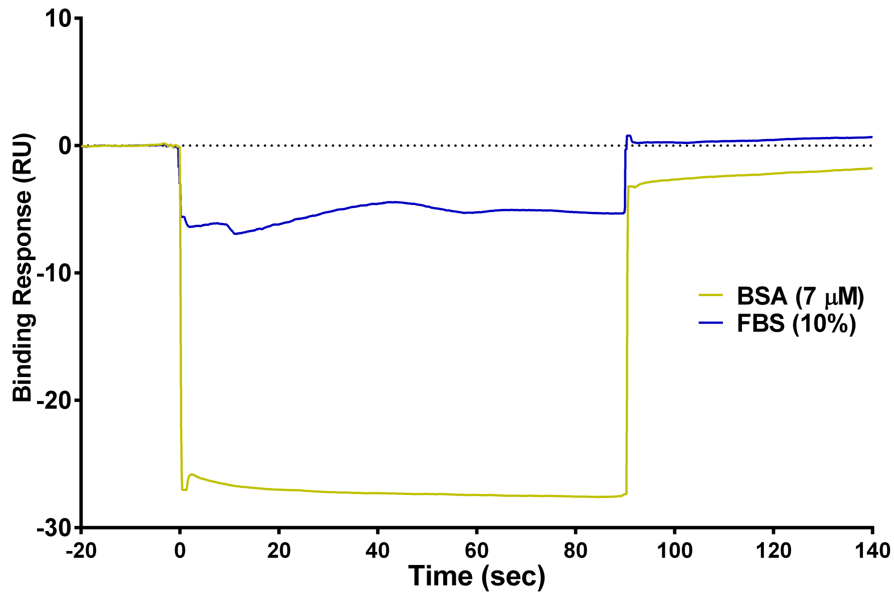

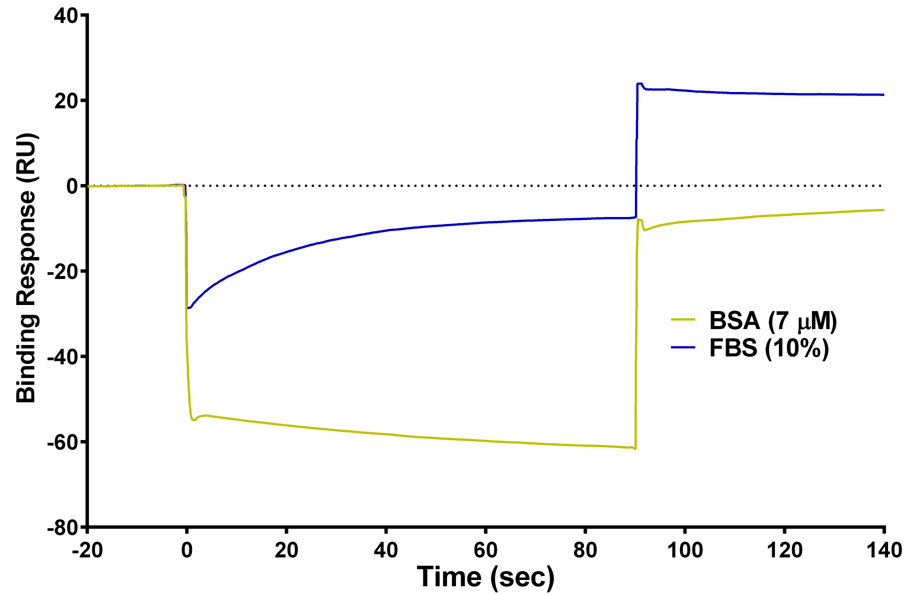

S11. SPR negative controls. Control BSA and FBS do not bind to TGFβR1 and TGFβR2.

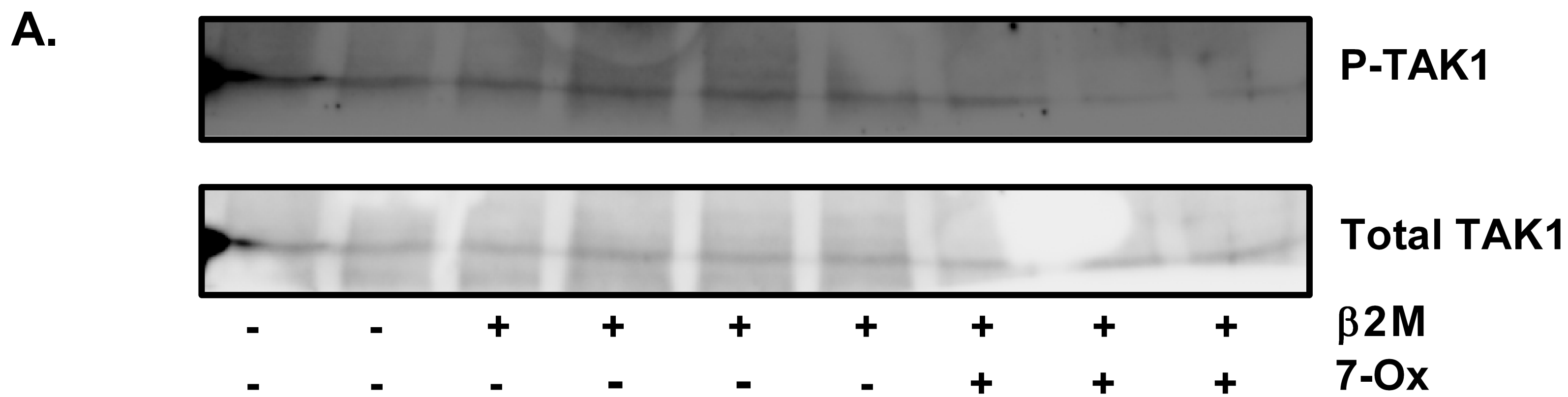

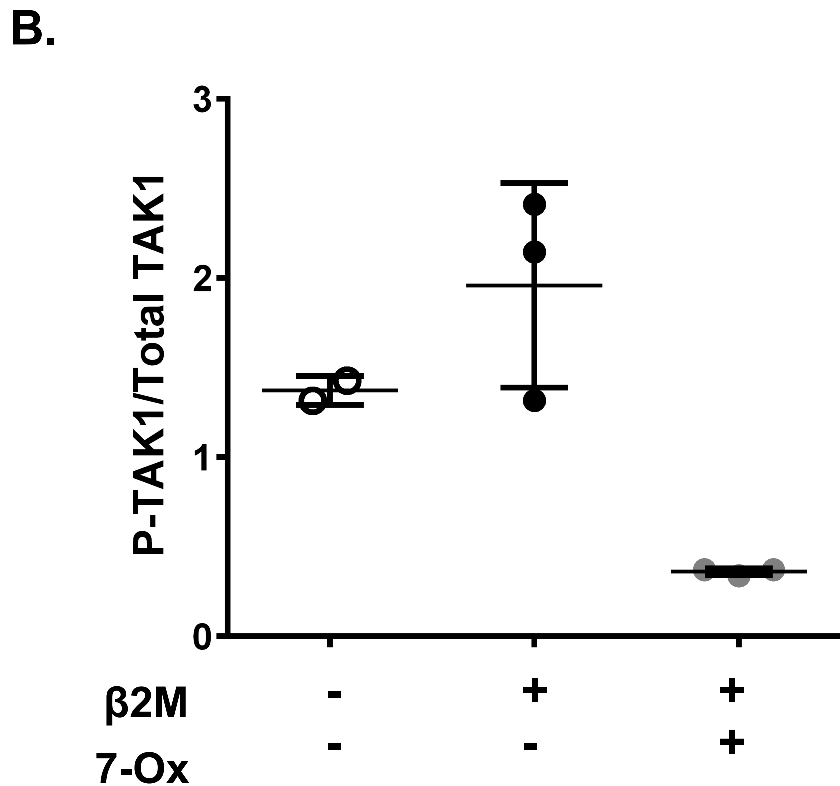

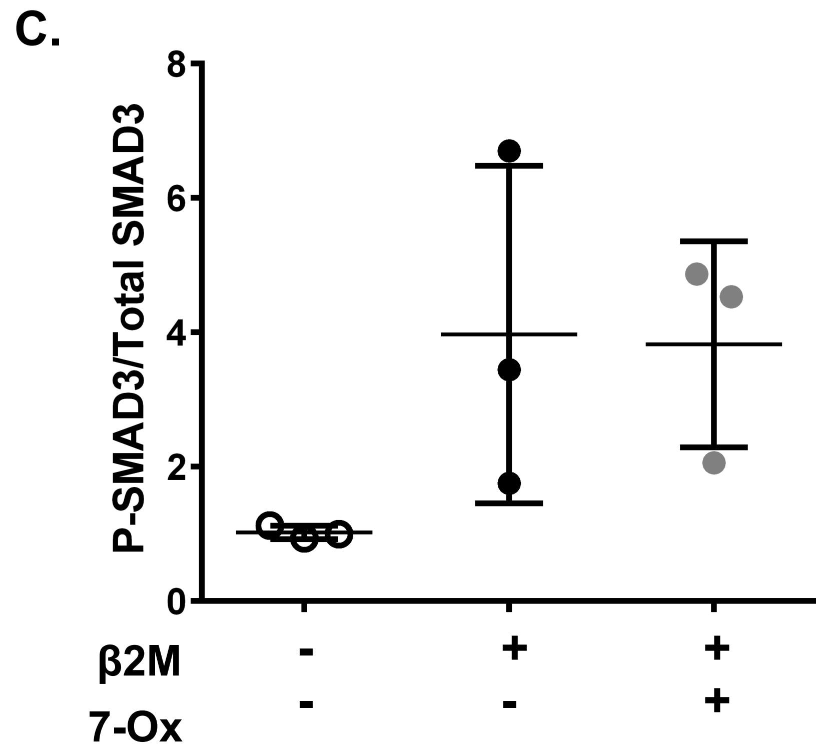

Fig S12. A) Immunoblot confirmation of TAK1 inhibition. B) Inhibition of TAK1 blocked β2M induced Tak1 phosphorylation (± SD), C) but does not blunt SMAD3 phosphorylation (± SD).

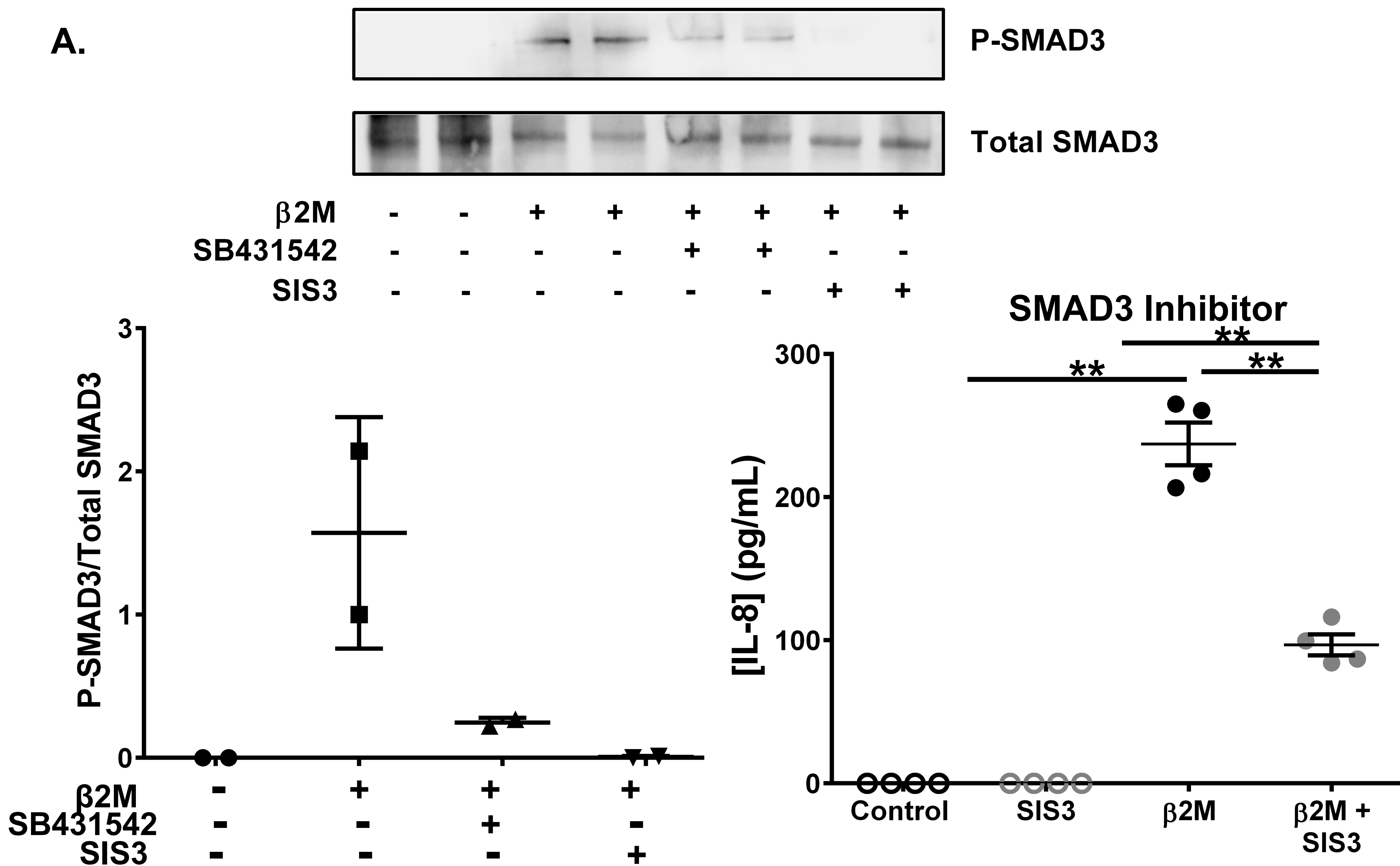

Fig S13. A) Immunoblot confirmation of SMAD3 inhibition. B) β2M increases phospho-SMAD3, that is inhibited by SB431542 and SIS3 (± SD). C) SMAD3 inhibition only partially attenuate β2M signaling as measured by IL-8 release (± SEM, one-way ANOVA with Bonferroni Correction) .

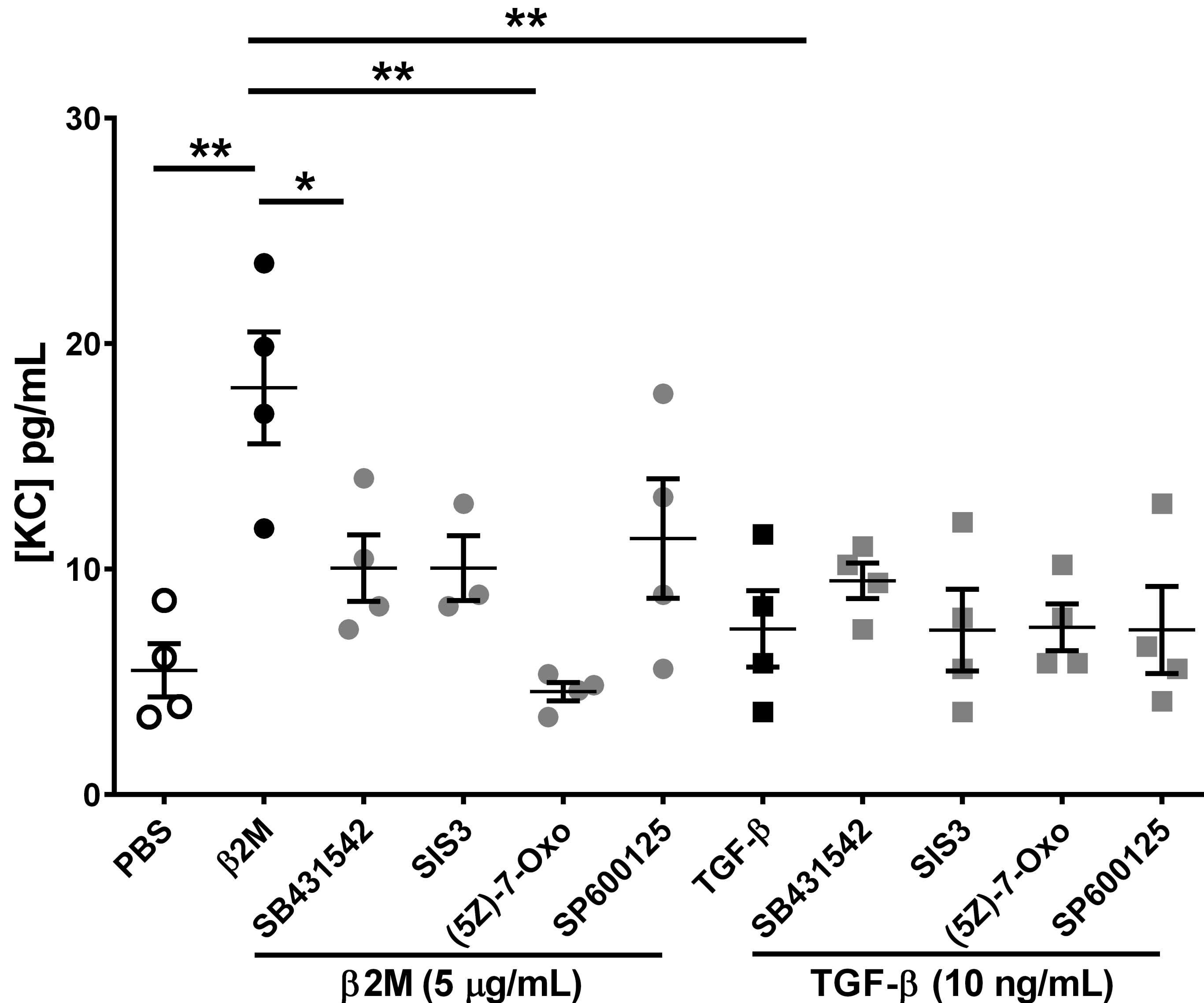

Fig S14. TGFβR→TAK1 signaling mediates mouse monocyte β2M responses (± SEM, **P<0.01, *P<0.05, one-way ANOVA with Bonferroni correction).

A.

pSmad2/3 (Fold Change Vs Control)

10 8 6 4 2 0

WT LysM-TGFβR2$^{-/-}$

B.

pJNK (% CD11b$^+$CD115$^+$)

30 20 10 0

Control β2M

C.

pSmad2/3 (% CD11b$^+$CD115$^+$)

30 20 10 0

Control β2M

S15. Intracellular flow cytometry. A) WT, but not LysM-TGFβR2$^{-/-}$ monocytes, responded to TGFβ (10 ng/mL; ± SEM, *P<0.05, one-way ANOVA with Bonferroni correction). B-C) β2M induced P-JNK and P-SMAD2/3 in primary mouse monocytes. P-JNK and P-SMAD2/3 measured by intracellular flow cytometry after 5 µg/mL β2M treatment (± SEM, *P<0.05, one-way ANOVA with Bonferroni Correction). D. TAK1 (7-Ox) and JNK (SP600125) inhibitors blocked P-JNK (± SEM, *P<0.05, one-way ANOVA with Bonferroni correction).

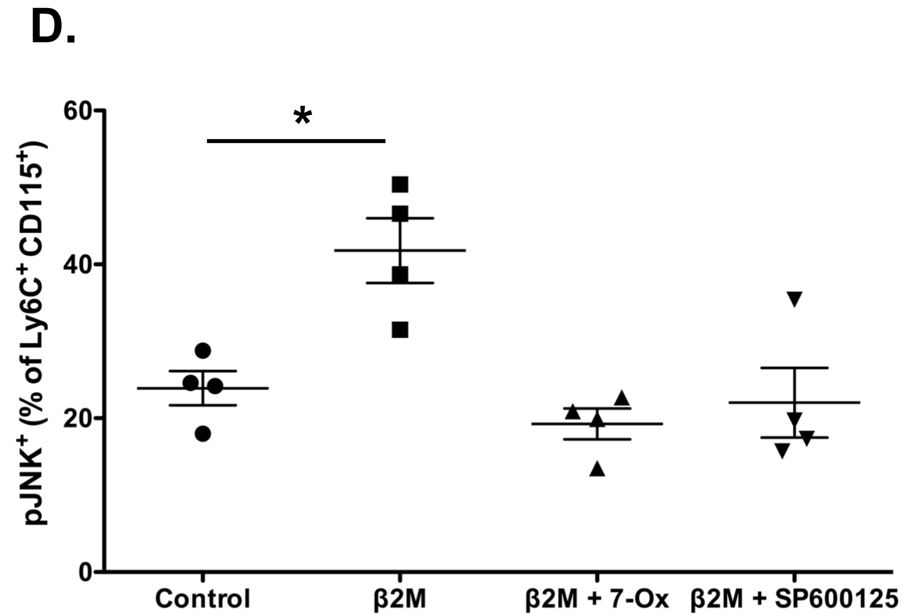

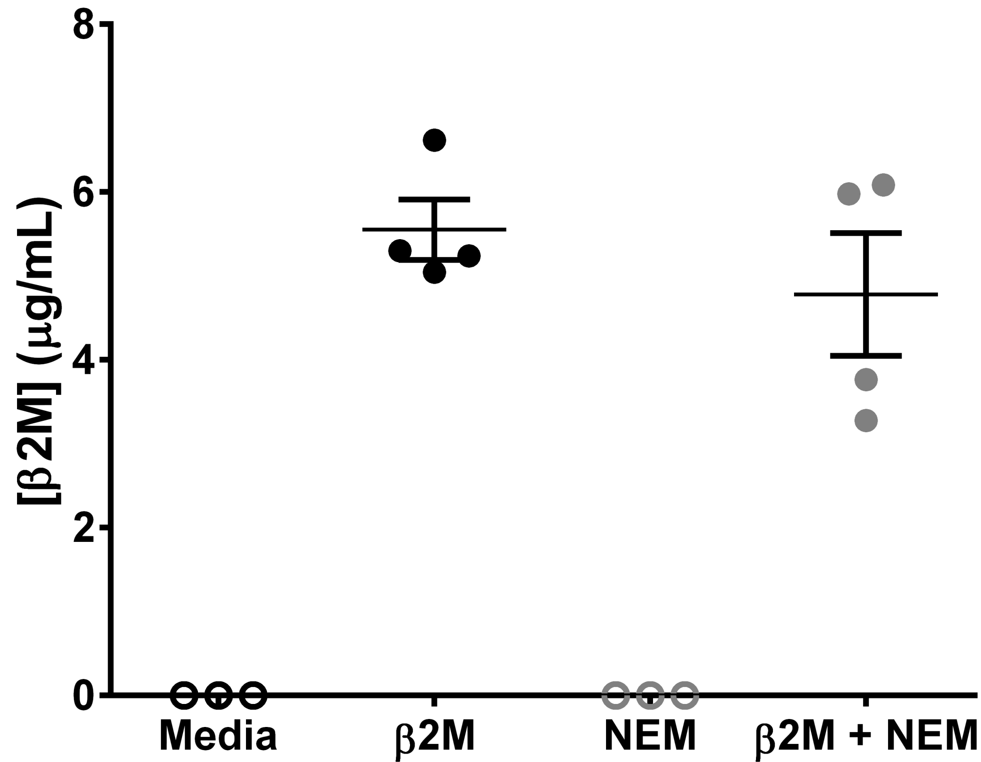

Fig S16. NEM multimer reduction does not alter recombinant β2M ELISA measurement (± SEM, one-way ANOVA with Bonferroni Correction).

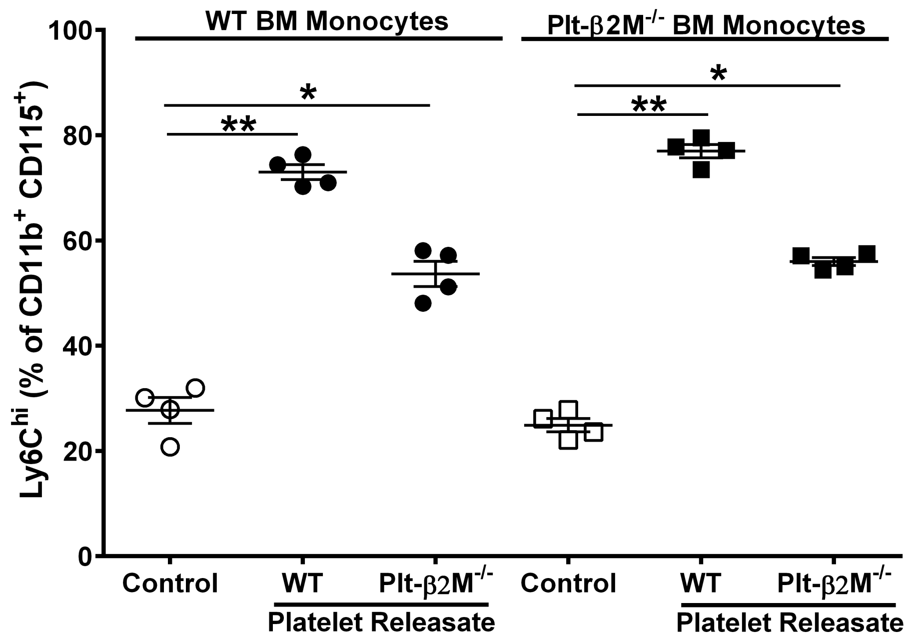

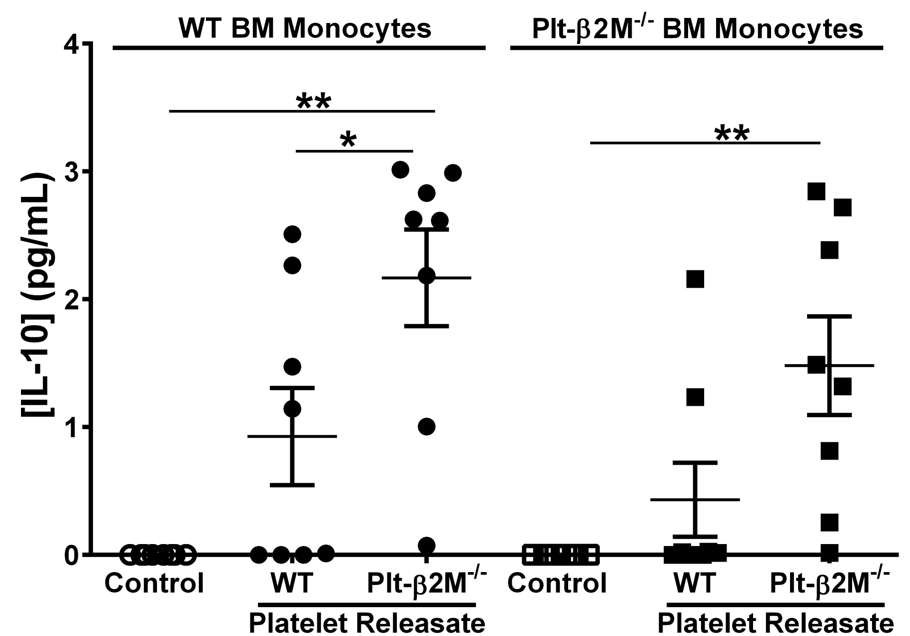

S17. WT and Plt-β2M$^{-/-}$ mouse bone marrow monocytes have similar β2M dependent responses, indicating that β2M exerts its effects on monocyte differentiation in the periphery, not on monocyte bone marrow differentiation. A) WT and Plt-β2M$^{-/-}$ bone marrow monocytes upregulate Ly6C similarly in presence of platelet releasate (± SEM, *$P<0.05$, **$P<0.01$, one-way ANOVA with Bonferroni correction). B) A) WT and Plt-β2M$^{-/-}$ bone marrow monocytes release IL-10 in a similar manner (± SEM, *$P<0.05$, **$P<0.01$, one-way ANOVA with Bonferroni correction).

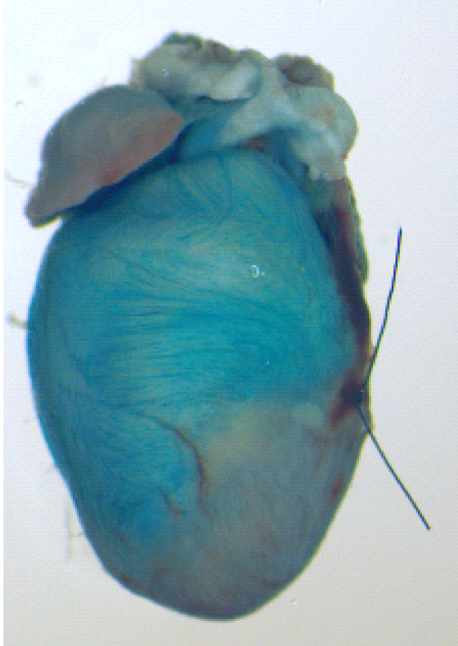

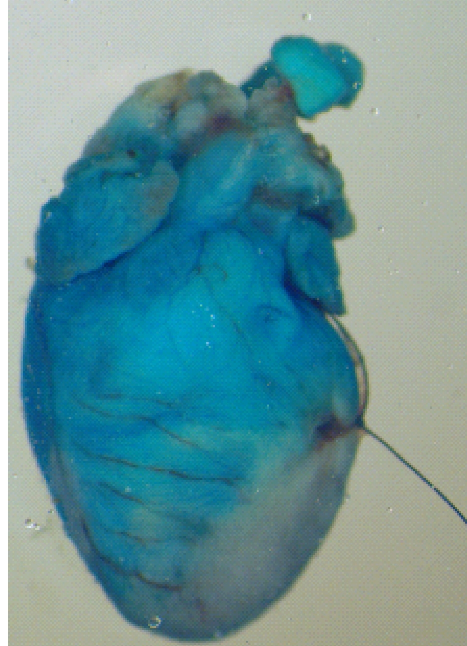

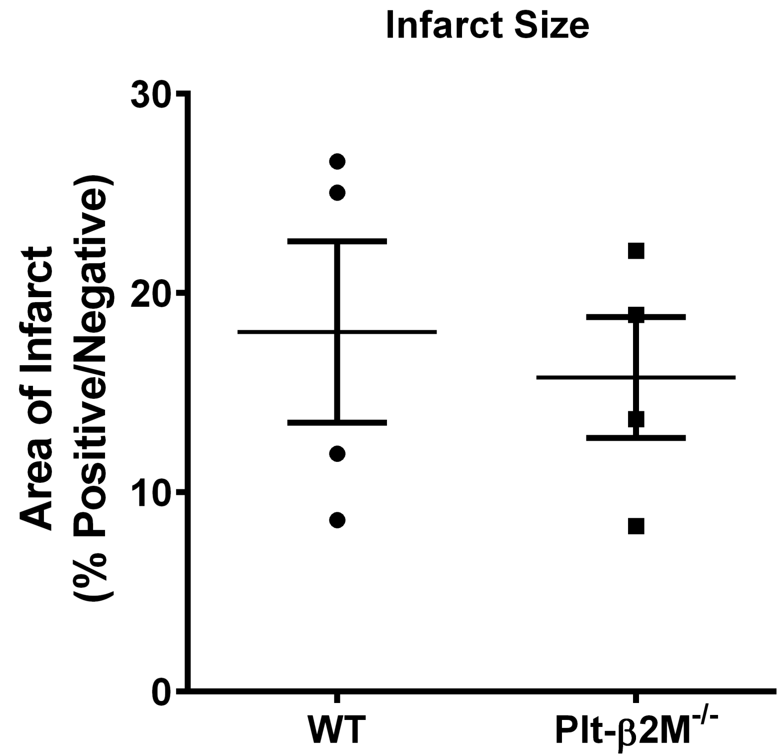

S18. WT and Plt-β2M$^{-/-}$ mice had similar infarct size. The LAD was ligated and mice injected with methylene blue dye. Infarct size was calculated as ratio of unstained vs stained heart tissue (± SEM, unpaired two-tailed t-test with Welch's correction).

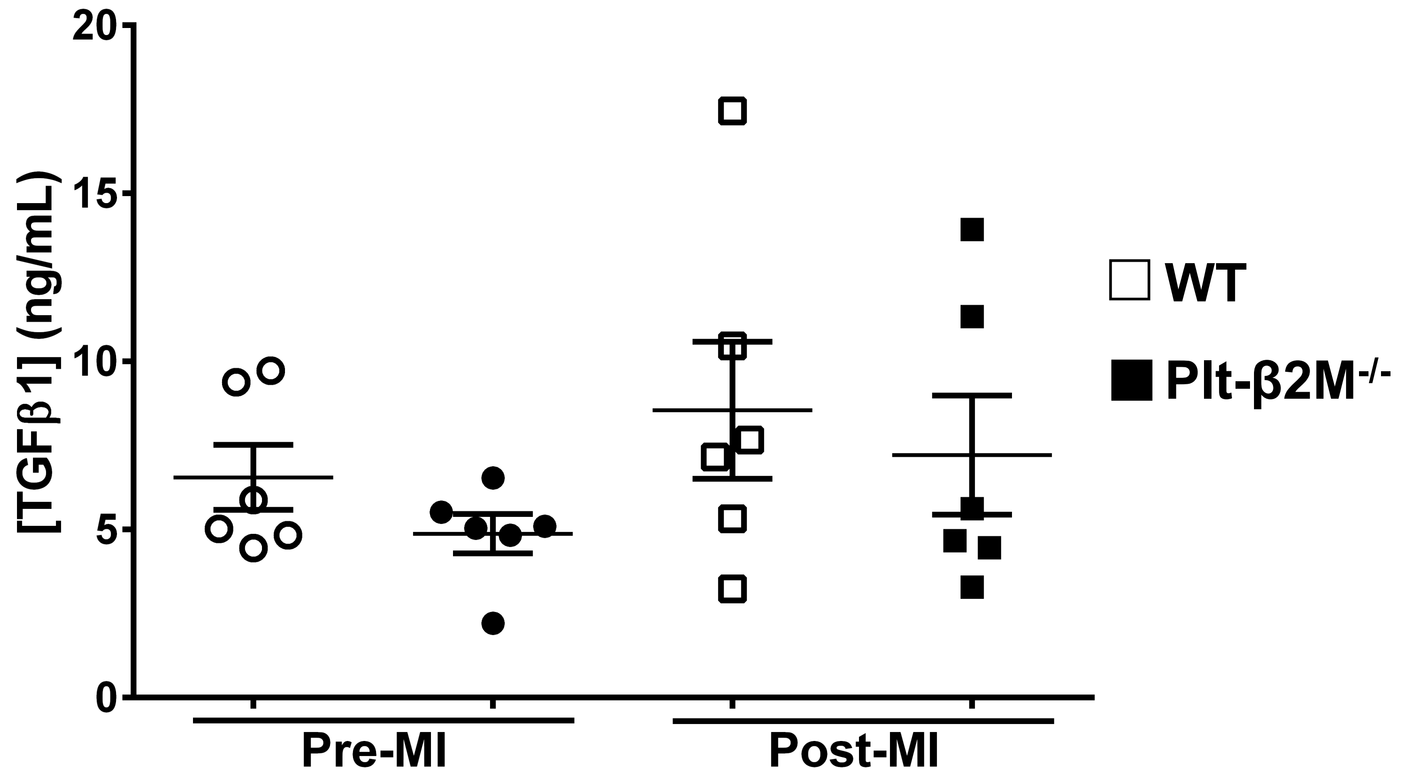

Fig S19. Pre and post-MI plasma TGFβ were similar in WT and Plt-β2M$^{-/-}$ mice (± SEM, one-way ANOVA with Bonferroni correction).

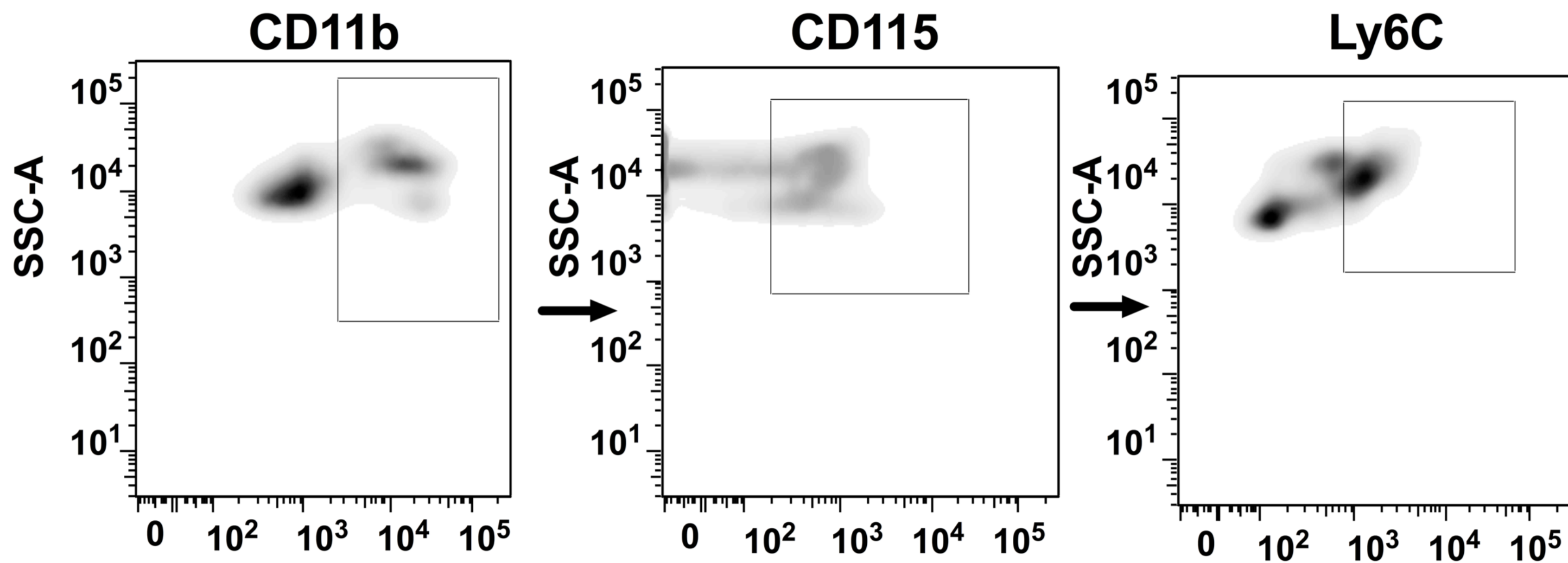

S20. Representative gating of peripheral blood flow cytometry.

WT **Plt-β2M$^{-/-}$**

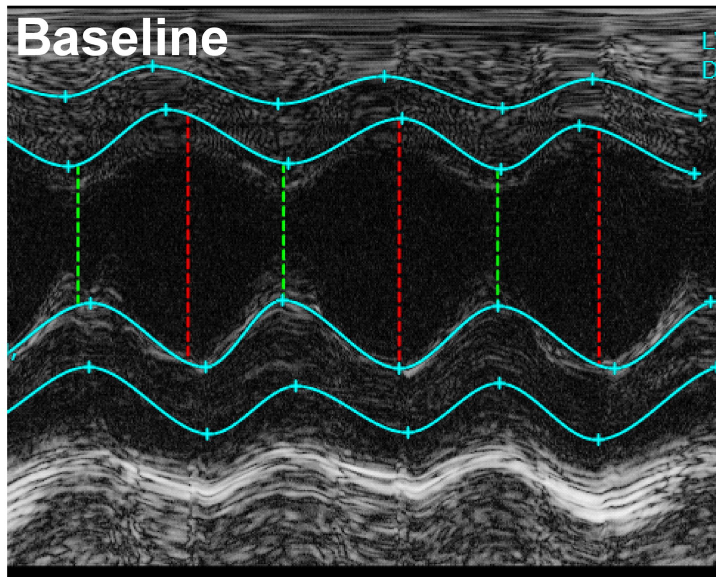

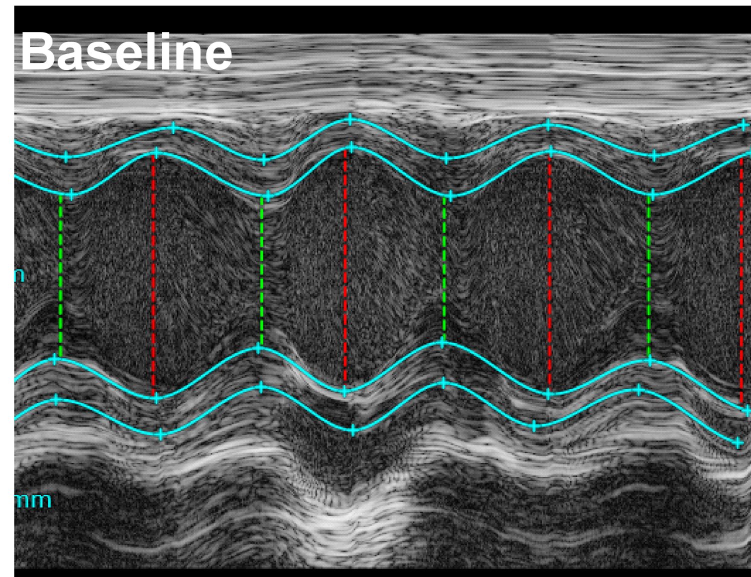

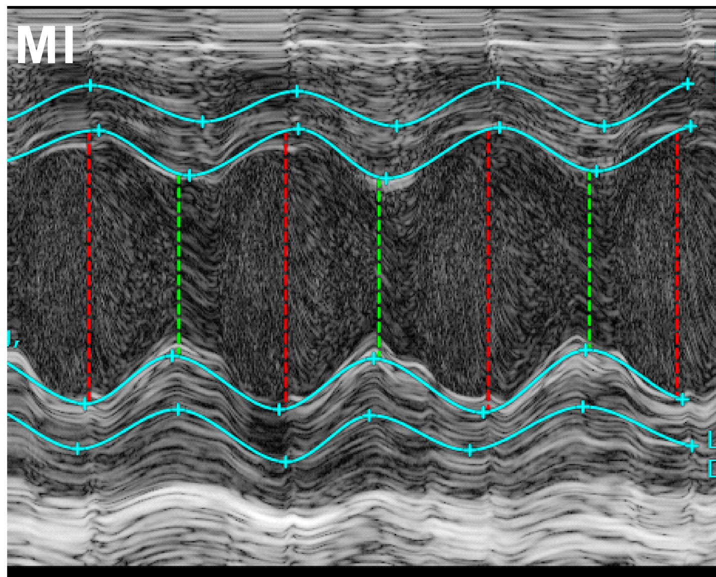

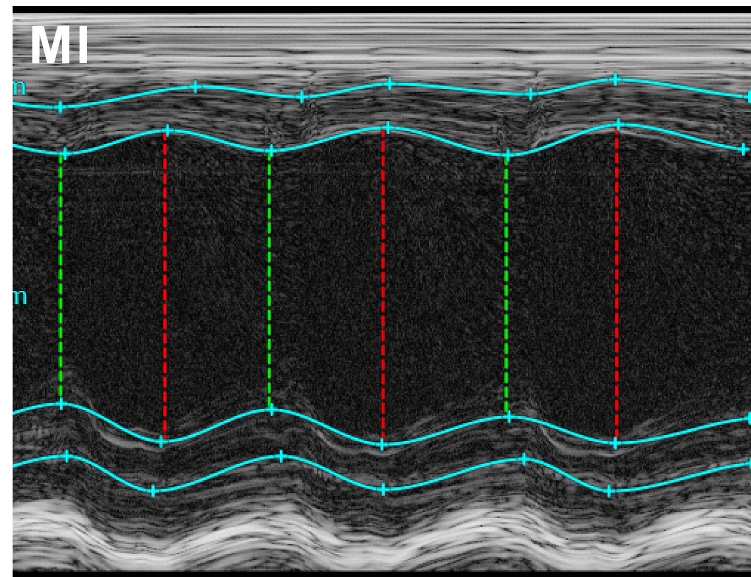

S21. Representative M-mode echocardiography.

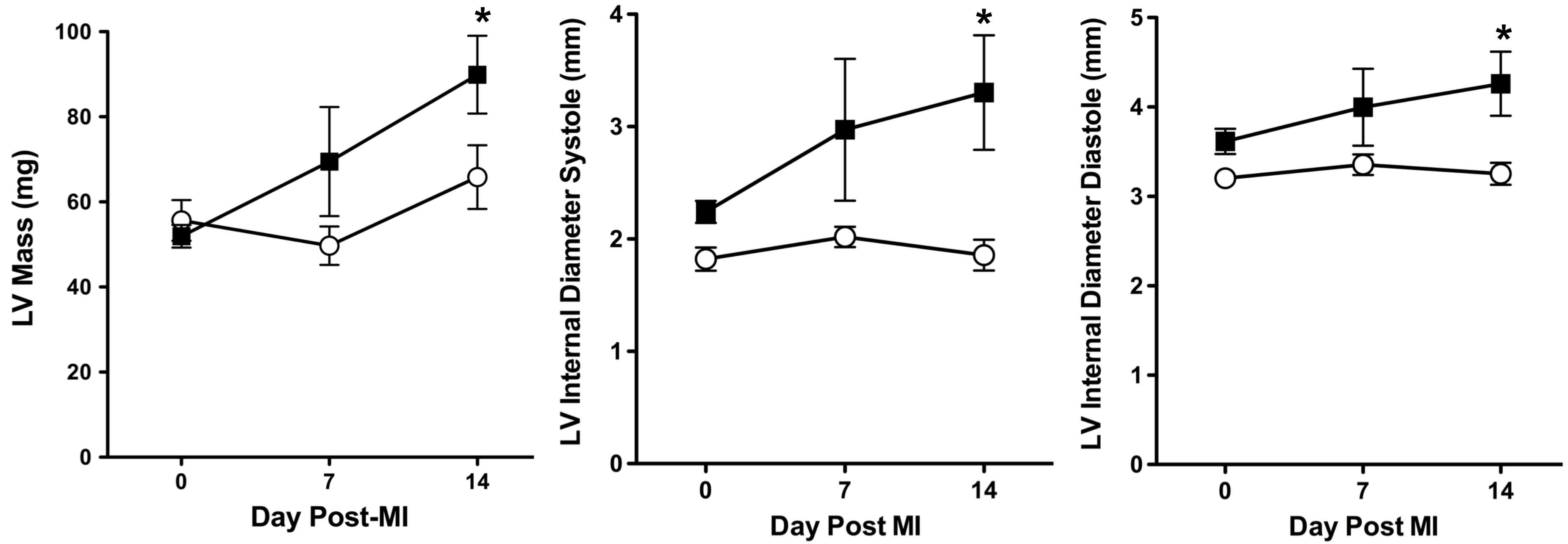

S22. Plt-β2M$^{-/-}$ mice had worse post-MI heart function compared to WT mice (± SEM, *P<0.05 vs WT, paired two-tailed t-test?).

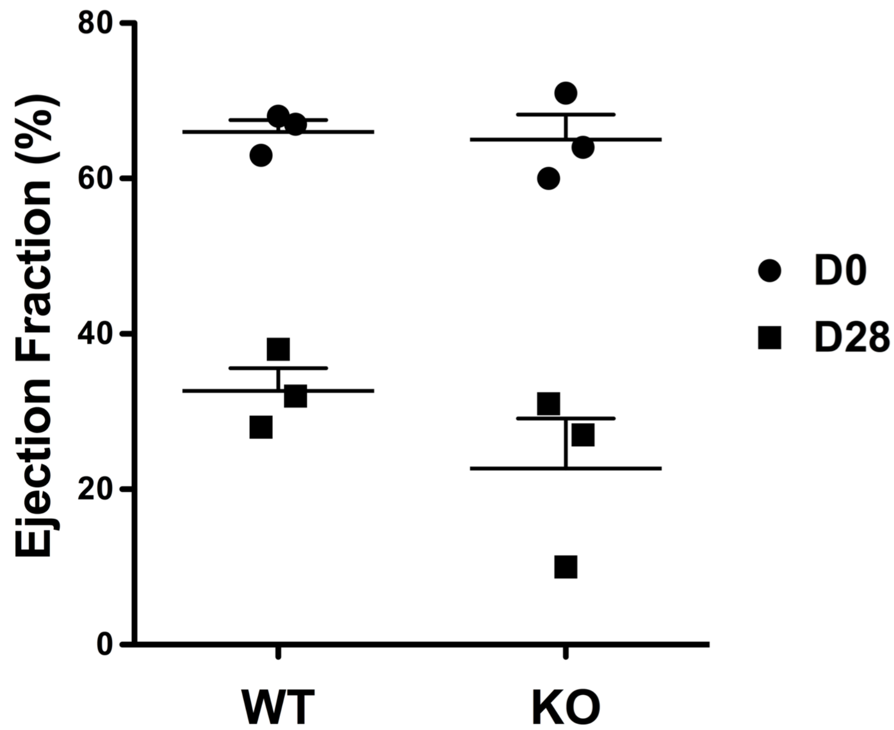

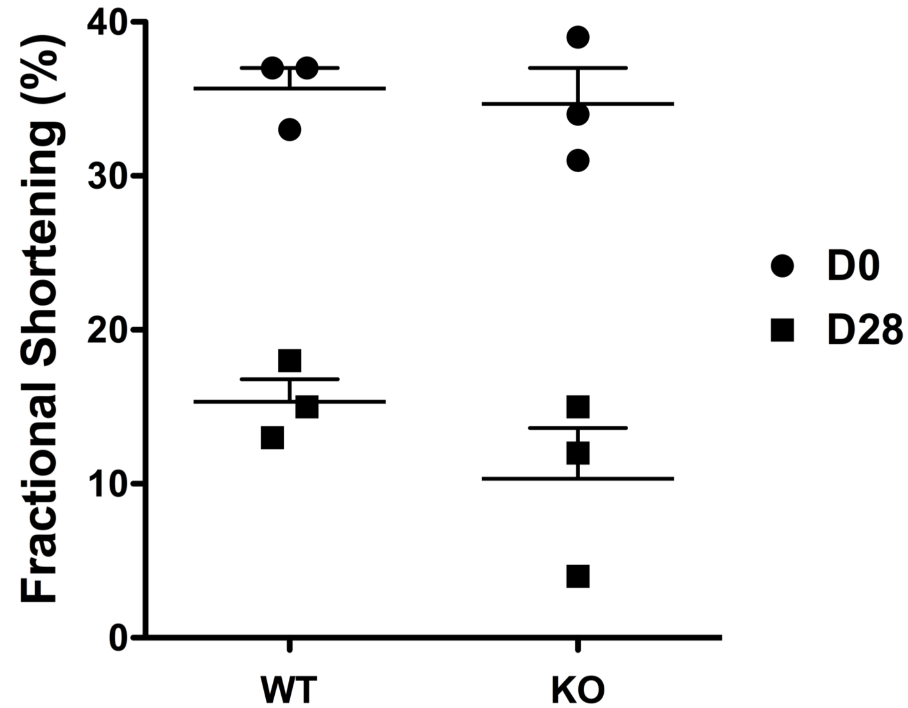

S23. Plt-β2M$^{-/-}$ and WT mouse heart function are more similar 4 wks post-MI compared to earlier time points (± SEM, paired two-tailed t-test).

Cell Type	WT N=6	Plt-β2M$^{-/-}$ N=6
WBC	10.55 ± 3	11.0 ± 3.2
Lymphocytes	5.7 ± 1.5	4.3 ± 1.1
Monocytes	0.54 ± 0.4	0.51 ± 0.42
Neutrophils	4.24 ± 1.9	4.8 ± 2.9
RBC	10.4 ± 1.4	10.4 ± 0.9
Platelets	730 ± 121	644 ± 106

S24. WT and Plt-β2M$^{-/-}$ mice had similar post-MI CBC (d7 post-MI, N=6, ± SEM, unpaired two-tailed t-test with Welch's correction).

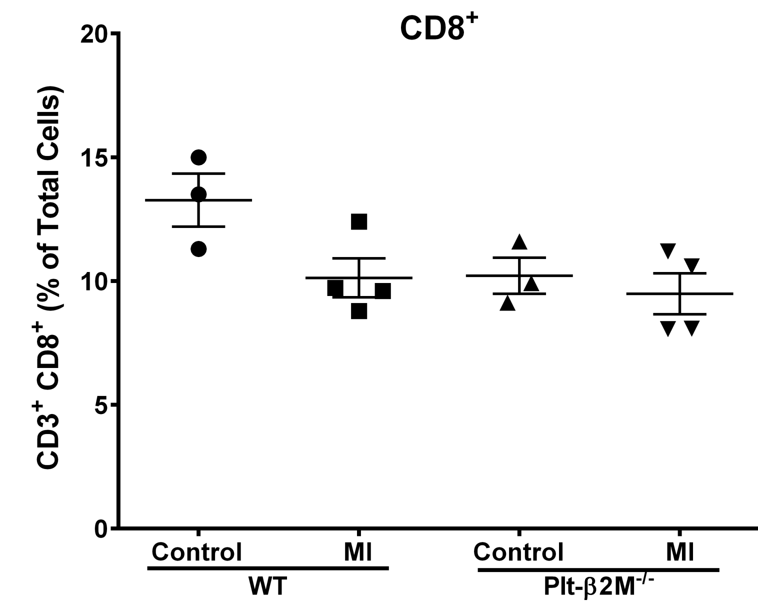

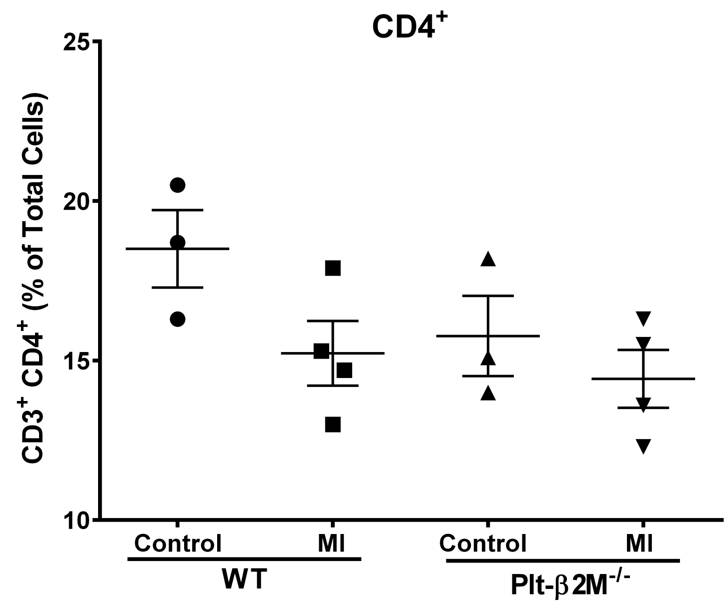

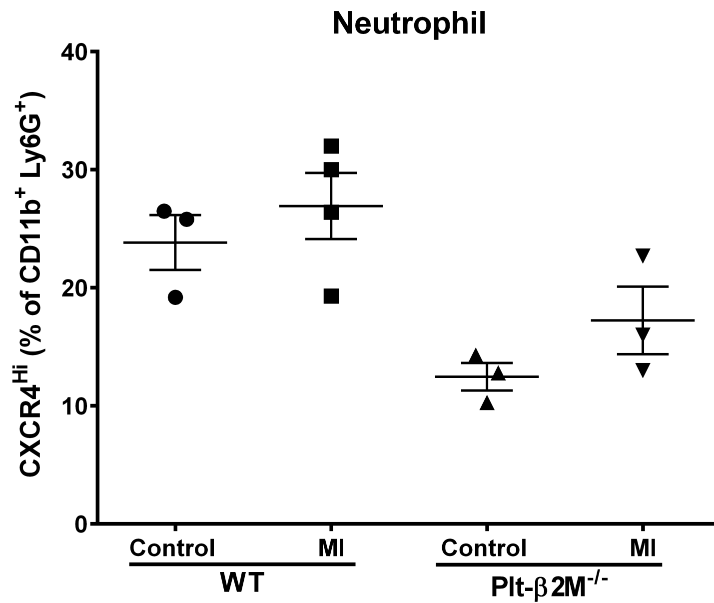

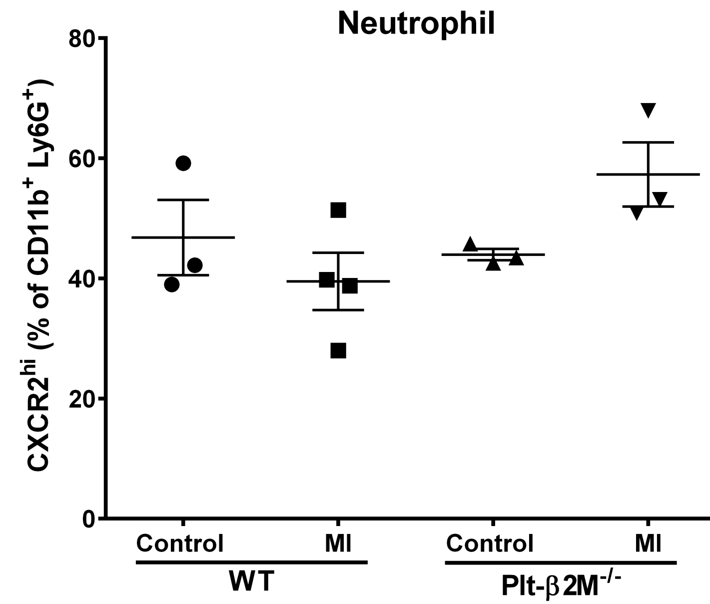

Fig S25. WT and Plt-β2M$^{-/-}$ mice have a similar d3 T cell and neutrophil responses.

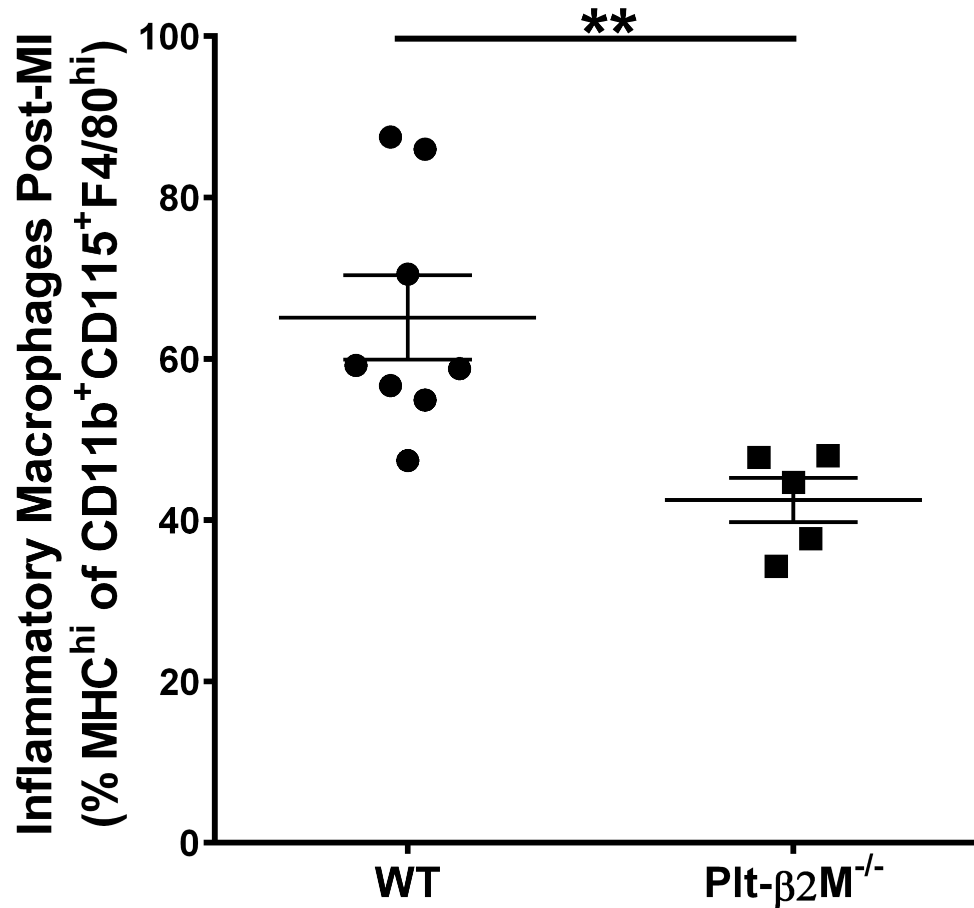

Fig S26. Hearts from WT mice on d3 post-MI had increased MHCII^{hi} (pro-inflammatory) macrophages compared to Plt-β2M$^{-/-}$ mice. Hearts were isolated from WT and Plt-β2M$^{-/-}$ mice on d3, collagen digested and macrophage phenotype determined by flow cytometry (± SEM, **P<0.01 vs WT, Unpaired two-tailed t-test with Welch's correction).

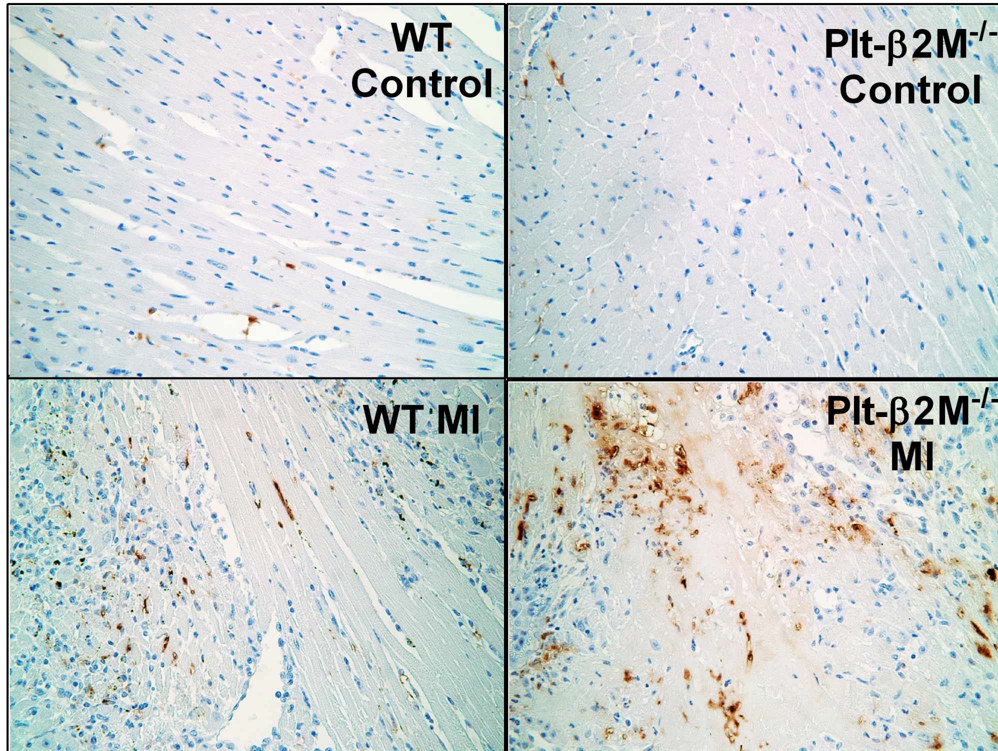

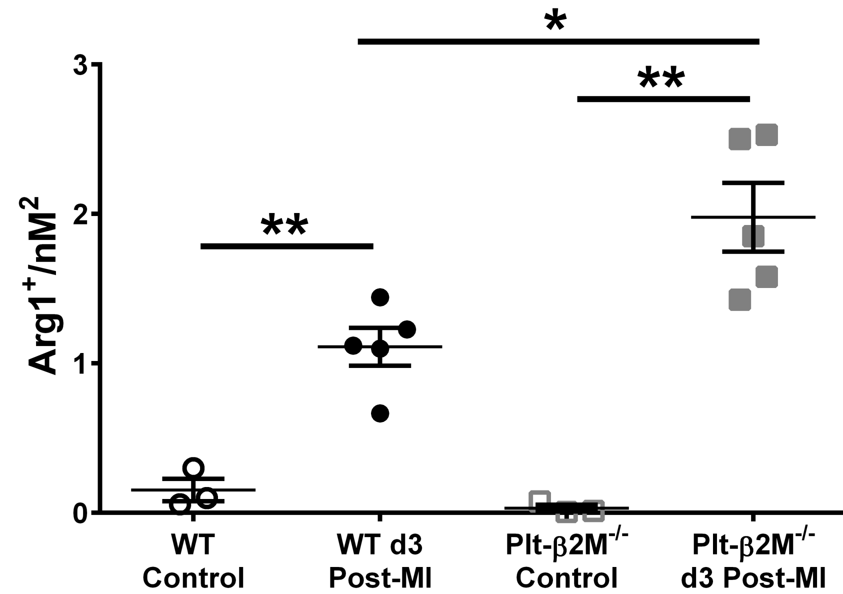

S27. Plt-β2M$^{-/-}$ mice have more Arginase-1 positive infiltrates on d3 post-MI compared to WT mice. Representative 40x images and quantification (± SEM, *P<0.05, **P<0.01, one-way ANOVA with Bonferroni correction).

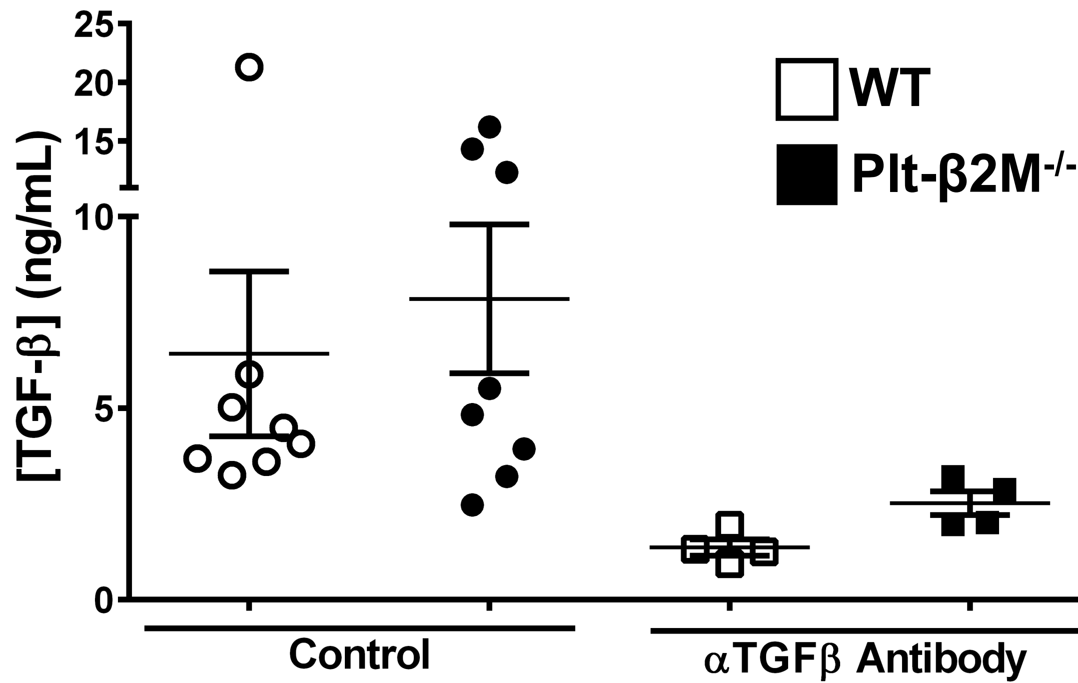

S28. Anti-TGFβ antibody reduced circulating plasma TGFβ in both WT and Plt-β2M$^{-/-}$ mice at d4 post-MI (± SEM, one-way ANOVA with Bonferroni correction).

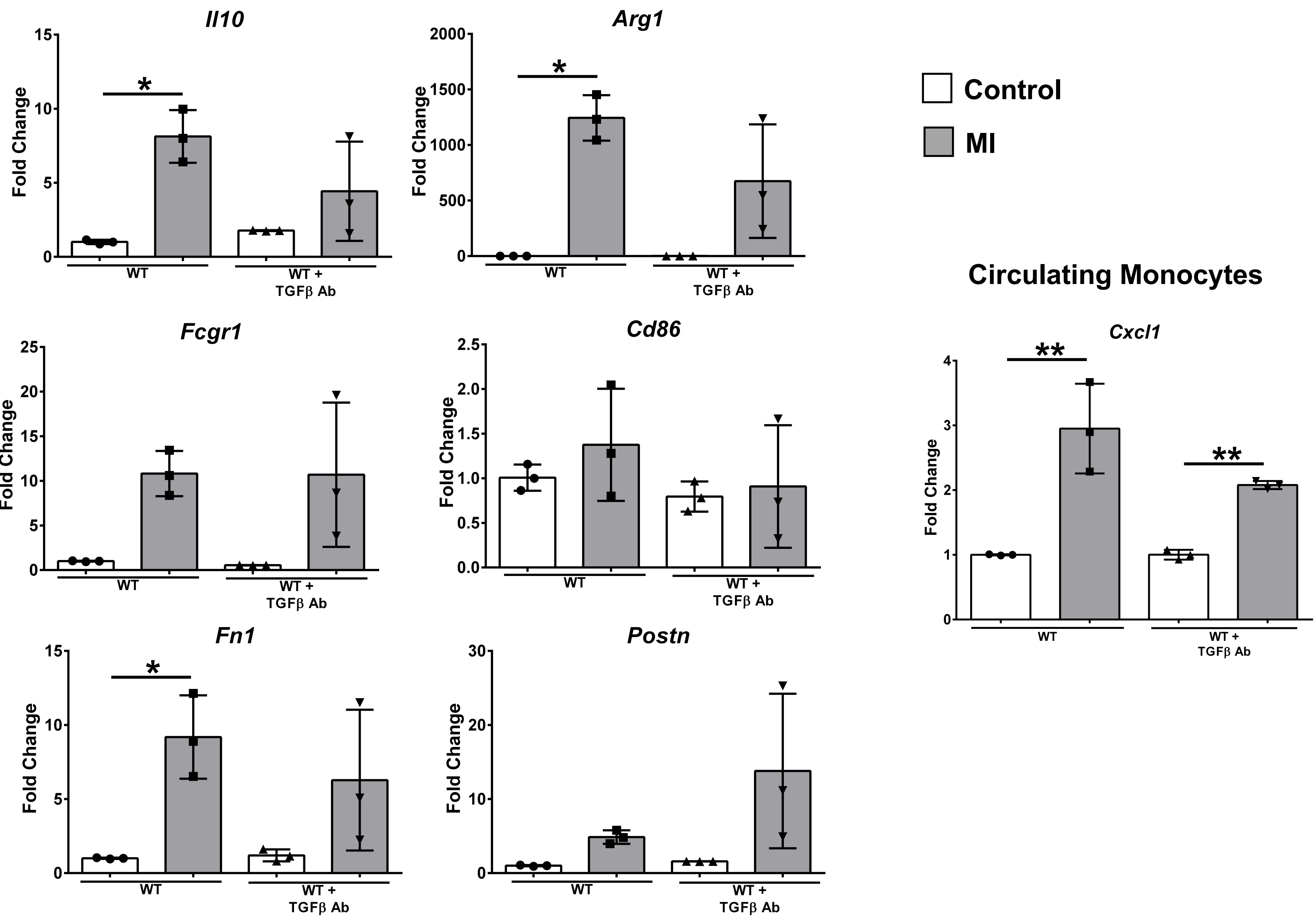

S29. Anti-TGFβ antibody treatment did not change the monocyte and macrophage phenotype of WT mice at the early d4 post-MI time point (± SEM, *P<0.05, **P<0.01, one-way ANOVA with Bonferroni correction.